Vapor Recovery Technique for Crude Oil Ship Loading —Spray Absorption[†]

SHIBUYA Yoshiki[*1]

Abstract:

In petroleum exporting countries, exhaust gas from crude oil tanker through loading operation at offshore terminals is the serious pollutant. A spray absorber, which is not affected by pitching and rolling motions in a floating plant, will be key equipment for the vapor recovery from crude oil ship loading. Because there was no case to apply crude oil sprays for vapor recovery, a series of pilot tests had been conducted to confirm the performance of spray absorber. Crude oil vapor is very complex in nature and it makes the analysis of the pilot test result quite difficult. By focusing on butane, the performance evaluation was easily performed and the possibility to apply the spray absorber was suggested. A simplified model was proposed to trace the phenomena in the absorber, and it was proved that the performance could be simulated by the calculations based on the model.

1. Introduction

Vapor exhausted while loading crude oil has become a serious problem in large-volume transportation of crude oil by tankers. As a large source of volatile organic compound (VOC) emissions, this tanker vapor has become a significant cause of environmental pollution, and it is known that the United States Environmental Protection Agency (EPA) has issued warnings about ground-level ozone originating from VOC pollution[1]. Particularly in the case of crude oils with high sulfur contents, bad odor caused by tanker vapor has an adverse effect on personnel working at shipping terminals. Moreover, gas also is also a waste of energy resources, as the released VOC includes components which are equivalent to liquefied petroleum gas (LPG) and gasoline. In 2007, JFE Engineering completed construction of the world's largest Tanker Vapor Recovery

System (hereinafter, TVR) at the Kiire Terminal of the Nippon Oil Staging Terminal (NOST). This paper describes a demonstration test of the spray absorption which is necessary when developing this technology to oil-producing countries.

2. Tanker Vapor Recovery System

2.1 Treatment Equipment at Kiire Terminal

The process flow diagram of the tanker vapor recovery (TVR) system at the Kiire Terminal is shown in **Fig. 1**.

Tanker vapor is transported to the TVR through vapor collection pipelines. In the TVR plant, first, the vapor is pressurized by a screw compressor, after which it is cooled and introduced into an absorber tower, which is filled with random packing. The crude oil, which is also used as an absorbent, similarly cooled and passed through the absorber tower. The vapor and crude oil are placed in contact in a countercurrent flow in the absorber, and the hydrocarbon component in the vapor is physically absorbed and recovered by the crude oil.
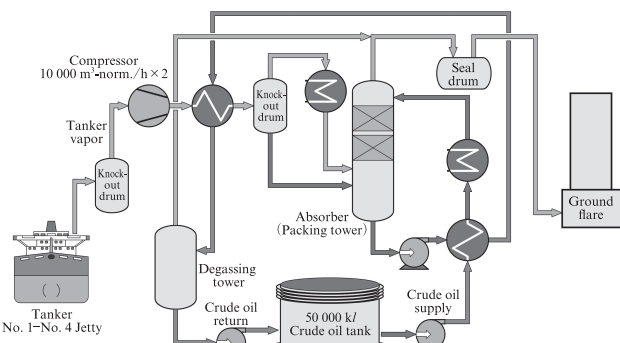

Fig. 1 Process flow of tanker vapor recovery (TVR) at Kiire Terminal, JX Nippon Oil & Energy Staging Terminal Corp.

[*1] Principal, Chemical Process, Plant Engineering Dept., Energy Industry Engineering Div., JFE Engineering

In recent years, the role of the Kiire Terminal as a crude oil relay stockpiling tank yard has become increasingly important for Japan. The vapor treated by the TVR System is collected from approximately 300 ships each year, centering on 100 000-ton class tankers. The energy recovered at the Kiire Terminal is equivalent to as much as 10 000 k*l*-crude oil/year.

2.2 Application to Oil-Producing Countries

As described above, while the TVR System is an environmental countermeasure facility, it also produces a significant profit by recovering energy. Application of this outstanding environmental technology in oil-producing countries which ship large volumes of crude oil is expected to contribute to technical progress in those countries and to assist in securing future sources of crude oil. In reality, however, a number of technical hurdles must be overcome in order to apply this technology in oil-producing countries. For example, although oil-producing countries ship large volumes of crude oil by tanker, the loading facilities are generally on offshore platforms or simple buoys such as single point mooring (SPM), and for this reason, it is not possible to secure a site for installation of a TVR plant. Therefore, JFE Engineering, in a tie-up with Universal Shipbuilding Corp. (now Japan Marine United Corp.), conceived a method in which the TVR plant is constructed on a barge, which is then moored alongside tankers, and has proposed construction of marine plants, which can be accomplished at comparatively low cost. **Figure 2** shows a view of the proposed TVR plant on a custom-built vessel.

The problem in this method is the absorber tower. Because the TVR plant is installed on a barge in this type of floating plant, swaying caused by waves is unavoidable. The absorber tower, on the other hand, is an extremely large pressure vessel, with a diameter

Fig. 2   Custom build vessel for offshore tanker vapor recovery (TVR)

exceeding 3 m and a height exceeding 20 m. Due to its height, even slight motion at deck level will cause large-amplitude swaying at the top of the tower. Since the absorbent is supplied from the tower top, the inclination of the tower will cause a non-uniform downward flow, and it is also easy to imagine that the inertia of this reciprocal movement will slam the absorbent against the side wall of the tower. As a result, the absorbent will not properly utilize the surface area of the random packing, making it impossible to secure the liquid surface area necessary for absorption in the absorber tower. In recent years, the price of crude oil has remained high for an extended time. In response, producers have aggressively developed deep-water oil fields, and many floating production, storage, and offloading (FPSO) systems are now in operation. However, packed columns like the TVR absorber tower are not used in any of those systems[2].

As absorbers for use under strong swaying conditions, the spray tower and the cyclone scrubber are conceivable, but because the properties of crude oil differ greatly depending on the oil field, and there are also many unknowns in connection with the vapor, an absorber using the simplest spray method was assumed. In packed column absorber, optimum design of the absorber tower is possible based on data provided by packing manufacturers and the actual values measured at the Kiire Terminal. However, there are no precedents for vapor recovery by a spray tower system which atomizes crude oil, and the data necessary for design are also inadequate. Therefore, during FY 2012, a demonstration test of a spray absorber was carried out with the cooperation of JX Nippon Oil and Energy (NOE) and the Nippon Oil Staging Terminal (NOST).

3. Test Plant

3.1 Outline of Spray Absorber Test Equipment

The spray absorber test was performed using actual vapor-absorbing crude oil and tanker vapor at the Kiire Terminal. An outline of the spray absorber demonstration test equipment is shown in **Fig. 3**.

The spray absorber is a horizontal cylindrical pressure vessel with an inner diameter of 500 mm. The crude oil vapor is passed in the horizontal direction, and the liquid crude oil is spray-atomized downward from above. The spray nozzles comprise a large number of crosscurrent-flow absorbers arranged along the direction of the vapor flow. In the figure, the vapor is introduced from the left side of the absorber and flows to the right at a low flow velocity. The liquid crude oil is atomized by the large number of nozzles from above and placed into direct contact with the vapor. The spray nozzles are

Table 1 Spraying data of the emplyed spray nozzles

Model number	Spray angle			0.05 MPa		0.1 MPa		0.2 MPa (Standard)		0.5 MPa	
	0.05 MPa	0.2 MPa	0.5 MPa	Flow (l/min)	d32 (μm)	Flow (l/min)	d32 (μm)	Flow (l/min)	d32 (μm)	Flow (l/min)	d32 (μm)
020	60°	65°	55°	1.06	483	1.46	411	2.00	350	2.91	290
040	60°	65°	55°	2.12	579	2.91	493	4.00	420	5.81	348
060	70°	75°	65°	3.18	655	4.37	558	6.00	475	8.72	393

FR：Flow recorder　　　FG：Flow gauge
TR：Temperature recorder　PR：Pressure recorder
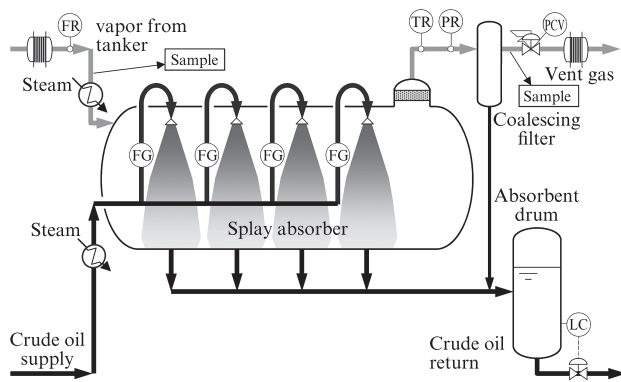PCV：Pressure control valve　LC：Level control

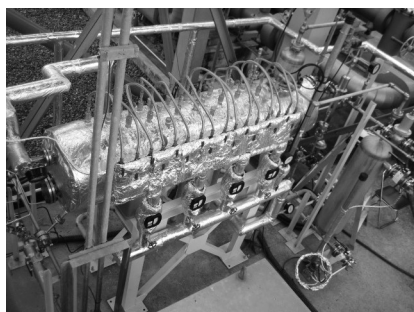Fig. 3　Field test apparatus for spray absorption

Photo 1　Overview Photo of the Test Spray Absorber

divided into 4 blocks, and the flow rate of each block can be controlled independently. In order to perform tests with a wide range of droplet sizes, mounting seats which enabled easy exchange of the spray nozzles were used. After absorption, the crude oil is discharged from

the bottom. The entrained oil mist in the vapor which has passed through the absorber is removed by way of a demister at the top of the discharge side.

As a precaution, a coalescer was installed on the downstream side in order to eliminate the entrained oil mist and prevent scattering to the downstream side. As test conditions, to enable operation at a temperature slightly higher than ambient temperature, heat exchangers were provided to heat both the vapor and the absorbent with steam before introduction into the absorber. A photograph of the test spray absorber is shown in **Photo 1**. For direct monitoring of the condition of atomization, one sight glass and another glass to let in light were provided in the absorber.

3.2 Spray Nozzles

The specification of the spray nozzle used in the test device is shown in **Table 1**. A standard full cone nozzle was selected for the spray nozzles. In case of typical hydraulic spray nozzles, a smaller nozzle has lower spray flow rate, and also makes finer spray droplet. Conversely, when the nozzle size is increased, both the flow rate and the spray droplet size increase, assuming spraying at the same pressure. When the same nozzle size is used, higher pressure gives higher flow rate and smaller droplet size.

3.3 Analysis and Recording

Vapor for use in analysis was sampled at the vapor inlet and exit, as shown in the flow diagram presented previously. The hydrocarbon (HC) content was measured by gas chromatography, and CO_2 content was measured by Orsat analyzer. For other data items such as the flow rate, temperature and pressure, etc., on-line sensor signals were recorded with a data logger.

4. Test Results

4.1 Outline of Results

In case of spray absorbers, process design based on the absorption equivalent to just one theoretical stage is normally conducted. However, sometimes the equilibrium of one theoretical stage might not be achieved due to the atomizing condition or other factors. As the result of this series of tests, the efficiency in HC recovery from tanker vapor was confirmed from the analysis data under a large number of test conditions, as shown in **Fig. 4**. In Fig. 4, the HC concentration of the inlet gas is shown on the x-axis, and that of the exit gas is shown on the y-axis.

In the absorption equivalent to one theoretical stage, the exit gas HC concentration depends on the inlet gas HC concentration and L/G (Liquid/Gas ratio), where L is liquid flow rate and G is gas flow rate. Under the test conditions shown by the plot points, L/G was expressed by darkness. The graph also shows the results of an equilibrium calculation by a process simulator under a temperature condition of 20°C. In many of the results with low L/G, the exit concentrations are higher than the calculated results, and they indicate the absorption
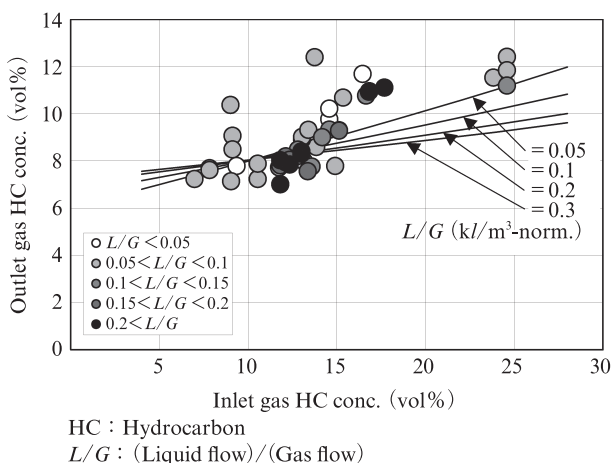
HC：Hydrocarbon
L/G：(Liquid flow)/(Gas flow)

Fig. 4　Overview of the test result

Fig. 5　Absorbed butane flow depends on feed butane flow

Fig. 6　Temperature effects on the performance

equivalent to one theoretical stage did not be achieved. On the other hand, when L/G is large, the exit concentration was sometimes lower than the calculated value. In such cases, it is supposed that the results were influenced by some factor other than L/G.

4.2　Detailed Confirmation of Results

For various reasons, analysis of absorption performance in a system comprising crude oil and crude oil vapor is extremely difficult. Analysis is difficult, for example, because in such systems, both of liquid and gas are mixtures containing many components, and depending on the case, not only the absorption but also the vaporization from the liquid, may occur due to the higher vapor pressure on the liquid side, etc. In this series of tests, the gas composition at both inlet and exit of the absorber was obtained as the gas chromatography analysis. This analysis was performed focusing on one composition, namely, butane (sum of i-butane and n-butane), which is the component with the largest absorption quantity. In **Fig. 5**, the flow rate of butane in the inlet gas is shown on the *x*-axis, and that of the recovered butane is shown on the *y*-axis.

When compared with the graph showing total HC, a quite good correlation can be seen. The primary regression line by the least-squares method is also shown. The relationship between the amount of inlet butane and amount of recovered butane shown here is scattered above and below the regression line as the mean. It is supposed that this expresses larger or smaller amounts of absorption, depending on differences in the test conditions.

Focusing on this deviation from the regression line, we attempted to identify some influential factors. Since temperature is highly influential on the gas-liquid equilibrium, this influence was investigated. A graph of the deviation with temperature on the *x*-axis is shown in **Fig. 6**.

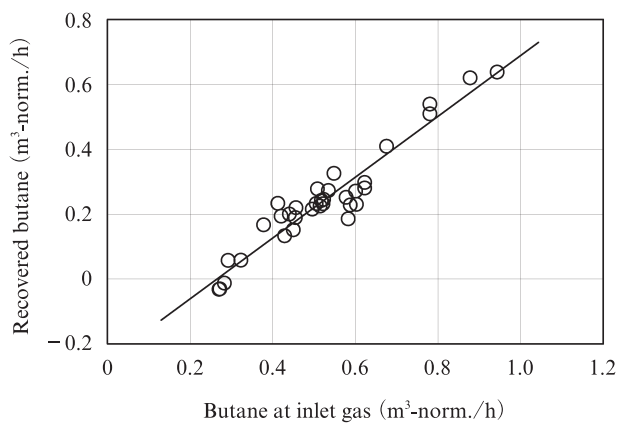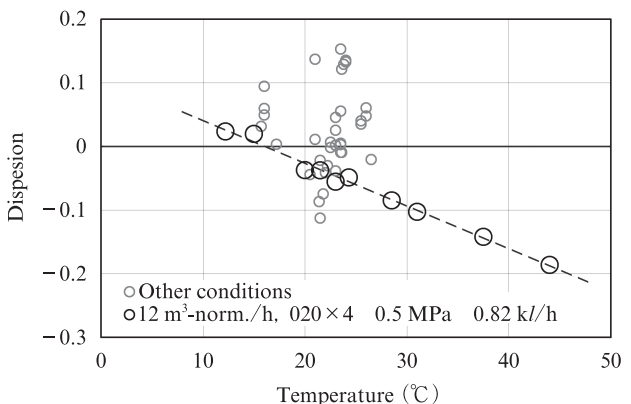Because the test conditions other than temperature

were same. A sharp correlation can be seen in the tests under various temperature conditions. It is obvious that temperature is the most influential. Moreover, in the tests conducted at ambient temperature, the temperature actually differed in the range from 12°C to 26°C. Therefore, this is considered to be a factor in the scattering of the results.

4.3　Comparison with Balance Calculation

In the simulation described above, the physical properties of the crude oil were modified, because they in the database of the simulator caused significant errors in the simulation. However, to know only butane equilibrium between gas phase and liquid phase of one theoretical stage, it can be a simple calculation according to Raoult's law or Henry's law[3].

Figure 7 shows the operating line of a theoretical stage with an equilibrium line according to Henry's law. The temperature of the liquid side is shown on the *x*-axis, and the partial pressure of the gas side is shown on the *y*-axis. Because the temperature and pressure were substantially constant in these tests, all these values were converted to butane content in gas, in order to simplify the comparison with the analysis values. In other words, on the gas side, partial pressure was con-
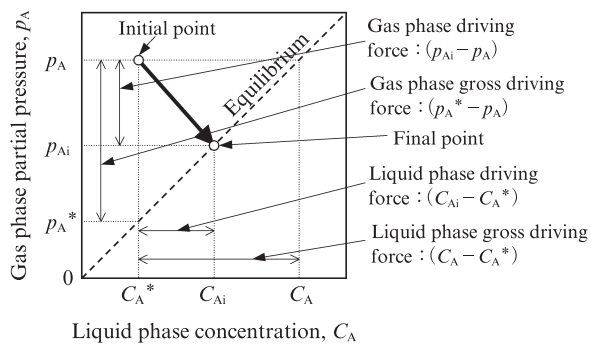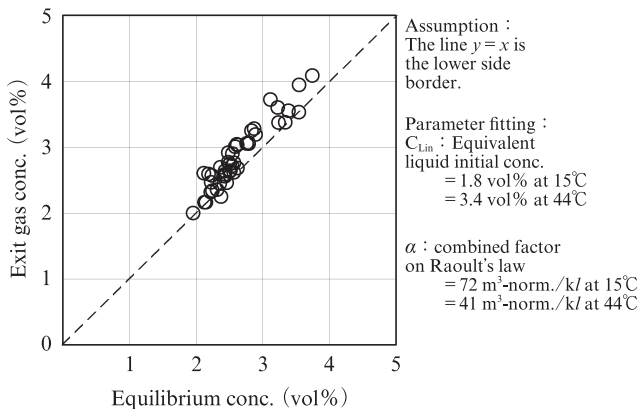
Fig. 7 Equilibrium solubility curve

Fig. 8 Calculated equilibrium conc. vs. Analyzed exit conc.

verted to concentration, and the liquid side was converted to the equilibrium concentration of the gas side corresponding to the concentration. α (m³-norm./kl) was defined as the equilibrium coefficient, and the equilibrium value C_{Geq} was formulated as follows:

$$C_{Geq} = \frac{C_{Gin} + C_{Lin} \times L/G \times \alpha}{L/G \times \alpha + 1} \quad \cdots\cdots\cdots\cdots\cdots\cdots\cdots (1)$$

In this equation, C_{Lin} and α were obtained by multi-parameter fitting.

In the test results under preferable conditions, the absorption shall almost reach to the calculated equilibrium value. Considering this fact, the parameters were defined so that the envelope of the plot may be in contact with the line where $y = x$. Furthermore, as described previously, because this is a gas-liquid equilibrium, temperature is the most influential factor. Therefore, both C_{Lin} and α were assumed to be linear functions of temperature. The results are shown in **Fig. 8**. The spray conditions and amount of absorption will be discussed in the next chapter.

5. Discussion

5.1 Theory of Spray Absorption

At the microscopic level, mass transfer by direct contact between a gas and a liquid is controlled by the diffusion on the gas side, the gas-liquid interfacial area,

and the diffusion in droplets, while at the macroscopic level, the important elements are the gas retention time and liquid holdup. In the case of a packed column, calculation methods are frequently established considering continuation of a steady state in a non-equilibrium condition. On the other hand, when studying direct gas-liquid contact by spraying, although the equipment is simple, the system is difficult, as an unsteady state solution is unavoidable.

Mass transfer at the droplet-gas interface and boundary layers has been studied based on an understanding of the motion of flying droplets and gas flow around the droplets[4], but it is difficult to measure and to estimate the condition of atomized crude oil droplet. Thus, many necessary values remain unknown. Moreover, it is almost impossible to explain the multi-component system of crude oil vapor and liquid crude oil by a strict model. Here, a simplified model is constructed, limiting the focus to the two elements which are indispensable in studying the spray absorption capacity: droplet retention time, and the mass transfer rate limited to butane on the droplet surface, and the calculated and actual values are compared.

5.2 Droplet Retention Time

When a liquid is discharged from a nozzle, it breaks up, forms droplets, and then undergoes continuing deceleration. This deceleration is frequently expressed by an equation of motion in which a sphere is decelerated by the resistance of air[5]. However, since this equation assumes that a spherical particle is not affected by other objects moving in a space where a gas is at rest, it would not be rational to apply this equation to the phenomena which occur during continuous spray atomizing. Although the kinetic energy which is lost to deceleration is received by the gas, if an extremely large number of droplets pass continuously through the gas, the surrounding gas will be accelerated, and within a short time, the velocity of the droplets and the velocity of the gas will become identical. The method of obtaining the velocity at which the kinetic energy comes into balance is much simpler than considering the motions of droplets microscopically, and can also provide a convincing explanation of actual motion.

The flow of gas in the system was modeled as shown in **Fig. 9** by dividing the space into the atomized region and non-atomized region. In the atomized region, the gas gains kinetic energy when the droplets are accelerated, and the gas loses kinetic energy by impact with the wall. In the vicinity of the nozzle, the gas is accelerated when the liquid flow breaks up, and thereafter, the gas continues to accelerate as atomization spreads and gas is drawn into the atomized region. Finally, it is assumed that the whole gas in the cross-sectional of atomized
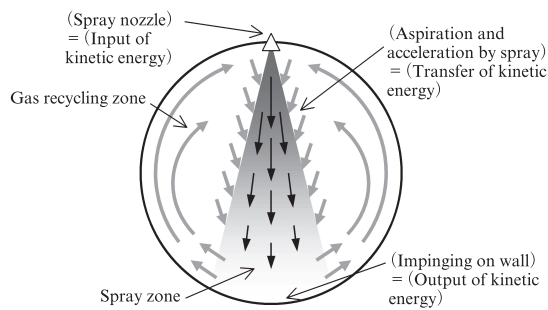
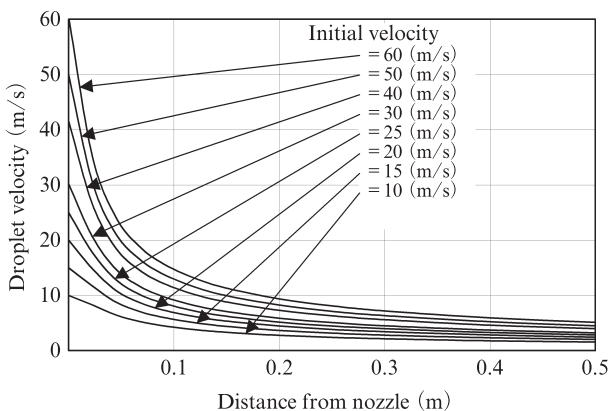Fig. 9 Model based on the balance of kinetic energy

Fig. 10 Calculated droplet velocity distribution

Fig. 11 Model of mass transfer

region reaches the same speed as the droplets immediately before impact with the wall, and an energy balance is achieved by this point. Although the droplets which impact on the wall are discharged downstream, the gas returns to the area around the nozzle by way of the non-atomized region.

If the kinetic energy at the outer side of the atomization region is ignored, and it is assumed that the gas reaches the velocity of the droplets at the instant of impact with the wall, the transfer of kinetic energy in the atomization region and the velocity at that time can be calculated in a simple manner. Although the results will differ depending on the spraying flow rate, an example of a calculation with a nozzle and absorber which are actually used is shown in **Fig. 10**.

When the curves in this graph are integrated, the retention time under the majority of the test conditions which were actually used can be estimated as being around 0.1 s. This result is also in good agreement with the result of an analysis of video images taken from the sight glass.

5.3 Simple Model of Spray Absorption

Visual observation confirmed that a gas which gains energy from a spray as described in the previous section is violently stirred. In this system, the retention time of the gas is several minutes, in contrast to the short retention time of the liquid of no more than 0.1 s, as mentioned above. Therefore, the condition is presumed as
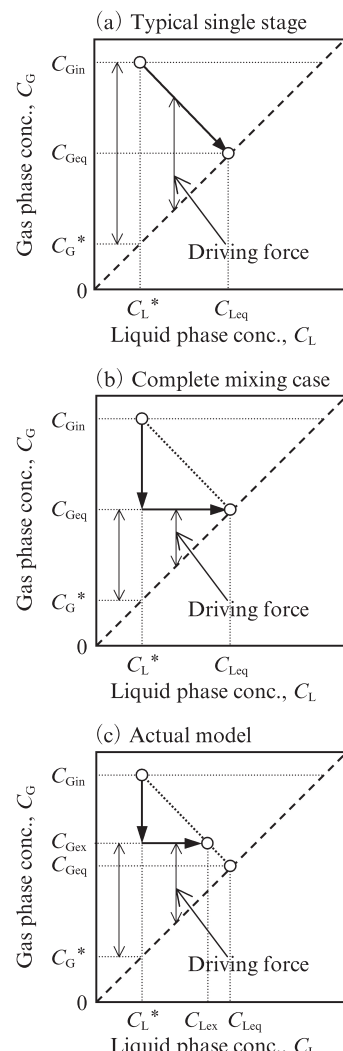
complete mixing. For this reason, it is assumed that the diffusion velocity of the gas is infinitely large and no concentration distribution exists. Furthermore, in self-washing-type gas absorption using the same liquid which is the gas generation source as the absorbing liquid (in this case, crude oil), the operating condition is generally characterized by an extremely large L/G ratio, and changes in concentration of the liquid are very small. Considering the fact that the droplets are small and the diffusion distance is short, it is assumed that the diffusion velocity in the droplets is also infinitely large and there is no concentration gradient within the droplets. Under these assumptions, it can be thought that mass transfer occurs in a certain entire volume on the gas phase, and in a certain elapsed time following atomization on the liquid phase, considering only the representative concentrations of the two phases. This simplified model is described below.

In **Fig. 11** (a), (b), and (c), a model of mass transfer is considered in a dissolution equilibrium diagram, with the concentration on the gas side C_G on the y-axis and the equivalent gas concentration C_L, in which the gas

concentration is converted to the liquid side, on the *x*-axis. First, Fig. 11 (a) shows the operating line for general absorption, as described above, rewritten as the equivalent gas concentration in this study. This is the theoretical operating line, assuming that the liquid and the gas flow in parallel streams, and there is sufficient time to achieve equilibrium. Since the initial driving force is large on both the gas side and the liquid side, efficiency is good. In contrast to this, if it is assumed that the gas side is completely mixed in the spray absorber, the concentration of the gas side reaches substantially the equilibrium concentration at the instant when the gas enters the system, and the driving force for mass transfer is reduced, as shown in Fig. 11 (b). However, in actuality, equilibrium is not achieved, and the concentration of the gas side becomes constant at an exit concentration which is higher than equilibrium, as shown in Fig. 11 (c). Under this condition, the driving force increases slightly. In any case, only the concentration of butane in droplets can change in this operation. This operation is performed in the short time from discharge of the liquid from the spray nozzle to impact with the wall. From the proportional relationship shown in Fig. 11 (c), the relationship between C_{Gi} and C_{Li} at a certain time is expressed by the following equation.

$$\frac{C_{Gi} - C_{Geq}}{C_{Gin} - C_{Geq}} = \frac{C_{Leq} - C_{Li}}{C_{Leq} - C_L{}^*} \quad \cdots\cdots\cdots\cdots\cdots\cdots\cdots\cdots (2)$$

In applying this model, assuming Henry's law is materialized, as described in the previous chapter, the concentration of butane in the crude oil side exists in a linear relationship with the concentration of butane in gas, which is in equilibrium, and can be handled by conversion. That is, if the subscripts G and L are treated in the same manner, then Eq. (2) can be expanded as follows.

$$C_{Li} = C_{Geq} - \frac{\left(C_{Gin} - C_{Geq}\right) \times \left(C_{Geq} - C_G{}^*\right)}{C_{Gin} - C_{Geq}} \quad \cdots\cdots\cdots (3)$$

However, as shown in Fig. 11 (c), the difference between the equilibrium concentration and the final concentration on the gas side acts positively in the driving force.

$$\begin{aligned} DF &= C_{Gex} - C_{Li} \\ &= C_{Gex} - C_{Geq} + \frac{\left(C_{Gin} - C_{Geq}\right) \times \left(C_{Geq} - C_G{}^*\right)}{C_{Gin} - C_{Geq}} \quad \cdots\cdots (4) \end{aligned}$$

Where, DF: Driving force (vol%)

In other words, as a model, the liquid side concentration is calculated assuming complete mixing and a uniform concentration on the gas side; however, in the equation, the gas side concentration is a simple term that

changes from the initial concentration to the final concentration.

5.4 Mass Transfer Coefficient

In analyzing test results by applying the above-mentioned model, the results of analysis at the gas inlet were used in C_{Gin}, and the results on the exit side were used in C_{Gex}. The $C_G{}^*$ used here is the equilibrium gas concentration, C_{Lin}, for the inlet concentration of crude oil obtained by fitting, as described in the previous chapter. In addition to this, the equilibrium concentration C_{Geq} was calculated by using the experimental condition of L/G and the value of α obtained by fitting in the previous chapter, and was assumed as the concrete value of the operating line. The mass transfer in a step time can be calculated by using Eq. (5) with the driving force obtained from these values, and the next concentration can be determined to perform the iterative calculation.

$$N = K \times S \times DF \times \Delta t \quad \cdots\cdots\cdots\cdots\cdots\cdots\cdots\cdots (5)$$

Where, N: Mass transfer in step time (m^3-norm.)
  S: Air-liquid interfacial area (m^2)
    (Water atomization equivalent)
  K: Mass transfer coefficient
    (m^3-norm./($m^2 \cdot$ vol% $\cdot$ s))
  Δt: Step time used in calculation (s)

The published droplet diameter in water atomization was used as the mean droplet diameter in spray atomization, and the gas-liquid interfacial area (water atomization equivalent) flowing in the system during a step time was calculated on this basis and used in the model calculations. In the calculations, the assumed value of the mass transfer coefficient and the setting value of the step time are necessary, but because a mutually inverse proportional relationship exists between the two, the product $K \cdot \Delta t$ of the mass transfer coefficient and the set step time was used in the calculation formula. Sequential computations beginning from the initial concentration where $C_{Gi} = C_{Gin}$ were then performed repeatedly, until the exit concentration where $C_{Gi} = C_{Gex}$ was achieved.

5.5 Verification of Model

The calculated results at 6 points in a typical example of a test under various spray conditions, etc. are shown in **Table 2**.

First, **Fig. 12** shows the process by which the retention time for traveling a distance of 500 mm was obtained by performing sequential computations of the droplet velocity using the above-mentioned energy balance under the respective spray conditions.

Besides this process, another sequential computa-

Table 2 Spraying data of the emplyed spray nozzles

Run number		1207B	1118I	1207A	1116E	1116L	1116M
Gas flow rate (m³-norm./h)		12.46	5.25	11.99	11.08	11.02	5.72
Spray rate	(kg/h)	0.35	1.64	0.9	1.66	1.24	1.24
Temperature	(°C)	17.2	24	16.2	23.5	23.6	23.6
Inlet C_4H_{10}	(vol%)	2.593	4.694	2.438	4.723	4.67	4.619
Outlet C_4H_{10}	vol%	2.163	2.563	1.999	2.631	2.761	2.64
L/G	(kg/m³-norm.)	0.028	0.312	0.075	0.15	0.113	0.217
Equilibrium conc.	(vol%)	2.149	2.414	1.957	2.504	2.571	2.285
Nozzle		020	060	020	040	060	060
Spray pressure	(MPa)	0.1	0.2	0.5	0.5	0.5	0.5
Initial velocity	(m/s)	30.2	41.6	60.4	60.4	60.4	60.4
Droplet diameter	(mm)	0.41	0.455	0.28	0.325	0.37	0.37
Spary angle	(°)	62	75	55	60	65	65

Fig. 13 Iterating calculation of mass transfer for each test

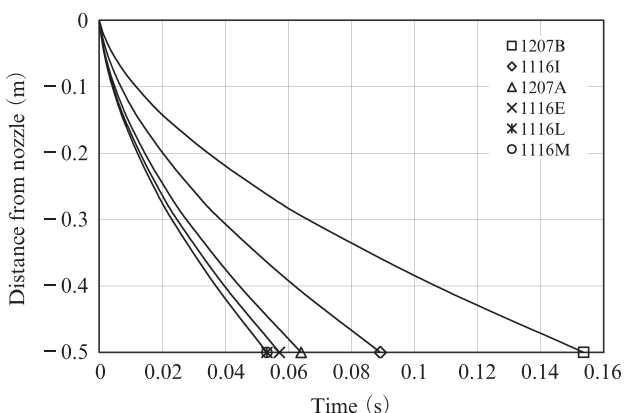Fig. 12 Retention time calculation for each test
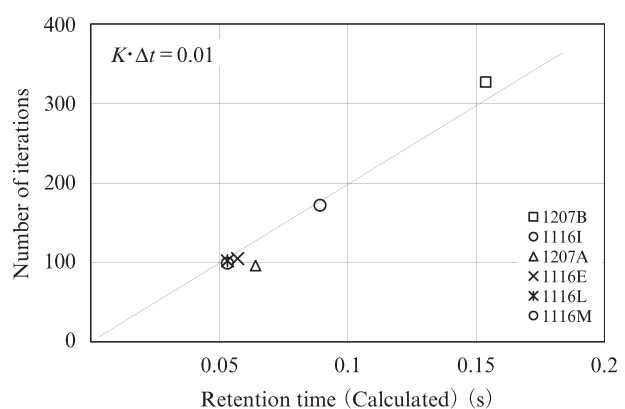
Fig. 14 Correlation between the number of iterations and retention tome

tions of mass transfer, in which the driving force was calculated at a constant gas side concentration, were performed with $K \cdot \varDelta t$ set to 0.01. Here, too, the condition in which the gas side concentration was absorbed from the inlet concentration to the exit concentration was plotted in **Fig. 13**.

In the sequential computation of mass transfer, the calculations were performed with many values, including the gas concentration, the flow rates of gas and liquid crude oil as test conditions, the mean droplet diameter in atomization, etc. Although these are data for various conditions, the time when the end-point is achieved showed a relationship similar to the previous droplet retention time. Therefore, the plots of the number of iterations until the exit concentration was achieved for this retention time are shown in **Fig. 14**.

As the calculated results at the 6 points shown in Table 2 are placed on a straight line passing through the origin, it can be understood that a proportional relationship exists between the retention time calculated by the energy balance model and the number of iterations of mass transfer by the complete mixing model. Since both sets of data are judged to have sufficient accuracy, mass transfer coefficients can be calculated from the graph. Moreover, because 300 iterations of the mass transfer
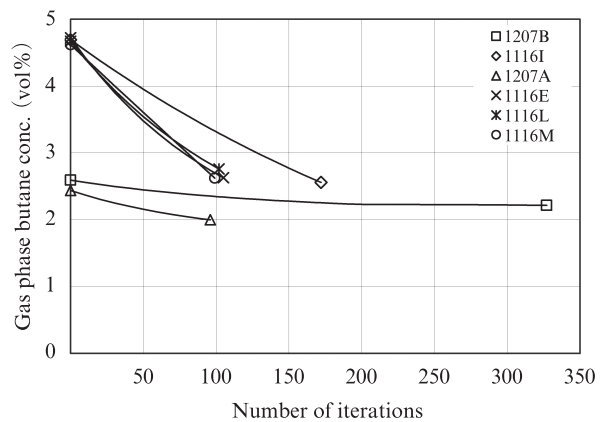
calculation is equivalent to a retention time of 0.15 s, the step time $\varDelta t$ of the iterative calculations is 0.000 5 s, and the mass transfer coefficient K is estimated as $0.01/0.000\ 5 = 20$ m³-norm. (m²·vol%·s).

Concerning the atomized droplet diameter, since the manufacturer's published value for atomization of water is used, the interfacial area equivalent to water atomization is used as the standard for the mass transfer coefficient. This research was successfully completed under this precondition. However, a future investigation will be necessary to determine whether the same evaluation can also be applied in case of different nozzle manufacturers or nozzles with different internal structures.

6. Conclusion

A simple, accurate mass transfer coefficient for the process of recovering hydrocarbons contained in crude oil vapor by spray absorption using crude oil as the absorbent was obtained by the method of (1) analyzing only butane as the object component, (2) obtaining the droplet velocity by a solution based on the kinetic energy balance, and (3) converting the concentration of the crude oil side to the equilibrium concentration for the vapor side, and calculating the mass transfer by a

simple model assuming complete mixing on gas phase. This method makes it possible to construct appropriate design standards for the design of large-scale equipment.

Finally, this demonstration test was conducted as part of "Study of Environmental Measures for Crude Oil Shipping Terminals in the Middle Eastern Region (Saudi Arabia)," which is one of Business Development Project for Commercialization in Oil-Producing Countries, and was carried out with the support of a Grant-in-Aid for Refining Technology, Etc. Measures for Oil-Producing Countries for FY 2012 provided by Japan Cooperation Center, Petroleum (JCCP).

References

1) "EPA Proposed Stronger Ground-Level Ozone Standards." Professional Safety. 2007, vol. 52, no. 8, p. 14.
2) Lapidaire, P.; Leeuw, P. "The Effect of Ship Motions on FPSO Topsides Design." Offshore Technology Conference 8079. Houston, USA, 1996.
3) Reid, R. C.; Prausnitz, J. M.; Poling, B.E. "The Properties of Gases and Liquids." 4th ed., McGraw-Hill, 1986.
4) Kugishima, M.; Nakajima, S.; Kunitake, M; Nagaoka, Y. "Development of an Operation Guide for Coke Oven Gas Refinery Process by Use of Absorption Droplet Model." Kawasaki Steel Giho. 1987, vol. 19, no. 2, p. 15.
5) Kajibata, Y.; Miwa, Y; Sakata, Y. "Development of Desulphurization Plants Using Spray Drop Simulation Model." Kagaku Kogaku Ronbunshu. 2006, vol. 32, no. 1, p. 59.